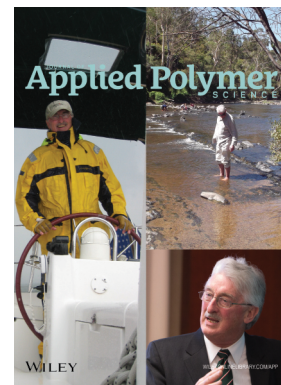## Special Issue: Sustainable Polymers and Polymer Science Dedicated to the Life and Work of Richard P. Wool

Guest Editors: Dr Joseph F. Stanzione III (Rowan University, U.S.A.)
and Dr John J. La Scala (U.S. Army Research Laboratory, U.S.A.)

Special Issue: Sustainable Polymers and Polymer Science
Dedicated to the Life and Work of Richard P. Wool

Guest Editors: Dr Joseph F. Stanzione III (Rowan University, U.S.A.)
and Dr John J. La Scala (U.S. Army Research Laboratory, U.S.A.)

Dynamic heterogeneity in epoxy networks for protection applications

Kevin A. Masser, Daniel B. Knorr, Jr., Jian H. Yu, Mark D. Hindenlang, Joseph L. Lenhart

U.S. Army Research Laboratory, Aberdeen Proving Ground Maryland

Correspondence to: J. L. Lenhart (E-mail: joseph.l.lenhart.civ@mail.mil)

ABSTRACT: The segmental dynamics and ballistic performance are investigated for a series of thermosetting epoxy networks composed of diglycidyl ether of bisphenol A (DGEBA) cured with mixtures of a rigid cycloaliphatic diamine and a series of flexible propylene oxide diamines. Formulations of DGEBA, cycloaliphatic diamine, and a low molecular weight propylene oxide diamine exhibit miscibility in the fully cured state, resulting in a single glass transition temperature (T_g), described by a Gordon-Taylor relationship. When high molecular weight propylene oxide diamines are used, the monomers are partially miscible, and the resulting cured epoxy exhibits dynamic heterogeneity, as evidenced by dual T_g's. These dynamically heterogeneous systems composed of rigid and flexible domains can exhibit enhanced ballistic impact response when the length scale of the phase separation is small, and the composition is near a phase inversion point. The dynamic heterogeneity also broadens the temperature window for impact performance, which is important for practical applications in military systems. © 2016 Wiley Periodicals, Inc. J. Appl. Polym. Sci. **2016**, *133*, 43566.

INTRODUCTION

Epoxy resins are utilized in a broad range of applications including adhesives and coatings as well as fiber and particulate reinforced polymer composites.[1,2] However, highly crosslinked epoxy networks are typically brittle. Quasi-static toughness of epoxy networks can often be improved by designing macroscale heterogeneity into the formulation including: incorporation of rigid or soft particulate fillers,[1,3–7] integration of phase separating rubbers,[8–10] development of interpenetrating networks,[11,12] or the formation of thermoplastic-thermosetting blends.[13–19] Here we investigate an interesting class of epoxy formulations that exhibit small scale heterogeneity. Most of these systems are not macrophase separated and are optically transparent, yet exhibit two glass transition temperatures, and are heterogeneous on a length scale approaching the size of individual monomers. We compare the ballistic impact resistance of these dynamically heterogeneous epoxy networks with both macrophase separated resins and homogeneous resins composed of similar monomers. The dynamically heterogeneous formulations exhibit high impact toughness over a broad range of temperatures which is important for military protection applications.

Dynamic heterogeneity, or the appearance of multiple T_g's within an otherwise miscible mixture, has been a subject of considerable research. Both thermoplastic and thermoset mixtures are known to exhibit dynamic heterogeneity, often in systems where the classic sign of heterogeneity is absent: macroscale phase separation.[20] The magnitude of the dynamic heterogeneity present in a given system depends on the difference in T_g of the neat components, as well as the thermodynamics of mixing, particularly the presence of specific interactions such as hydrogen bonds.[21] Understanding the existence of multiple T_g's or a single, broadened T_g in a composite material is important for practical applications given the broad operational temperature requirements for many manufactured parts.

The Twinkling Fractal Theory (TFT), developed by Richard Wool,[22–24] addresses several aspects of the glass transition. Of particular relevance to this investigation is its prediction of the effect of crosslinking density on T_g.[23] The TFT predicts that as the solid fraction of nanoscale domains percolates, the glass transition occurs. The TFT predicts T_g as a function of crosslinking density through the use of experimentally measured parameters and knowledge of the solid fraction at T_g. The ability to predict T_g as a function of crosslink density is critical when designing materials for a particular application. For the present investigation: mixtures of rigid and soft materials, a modification of TFT would be necessary to account for the mixture of crosslink densities in much the same way the Lodge-McLeish model[25] modifies the Fox-Flory rule of mixtures to account for self-concentration effects.

In this study, epoxy networks consisting of diglycidyl ether of bisphenol A (DGEBA) were crosslinked in stoichiometric amounts with mixtures of a rigid, high T_g and flexible, low T_g amine curing agent. It has been shown previously that DGEBA/PACM/D2000 and DGEBA/PACM/D4000 networks exhibit nanoscale structural

Figure 1. Chemical structures of the materials used in this study. For the Jeffamine series, "*n*" is approximately 2.3 for D230, 6 for D400, 33 for D2000, and 67 for D4000.
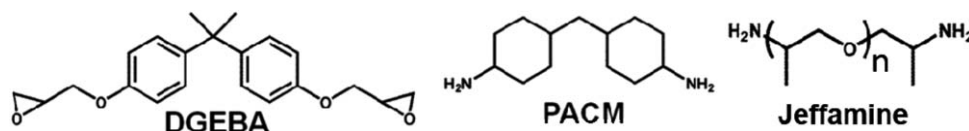
heterogeneity as well as dynamic heterogeneity.[26] Previously we showed that these nanostructured materials exhibit improved ballistic performance relative to epoxies formed with the neat components. In this paper, we expand upon previous work and investigate the effect of systematically changing dynamic heterogeneity within a series of mixed rigid and flexible diamine-cured epoxy resins. We define the ΔT_g as the difference in glass transition temperature between DGEBA crosslinked only with stoichiometric amounts of the rigid diamine (PACM) and DGEBA crosslinked only with stoichiometric amounts of the flexible diamine (D230, D400, D2000, or D4000). For mixed epoxy resins composed of both the rigid and flexible diamines, ΔT_g of the cured formulations was tuned by varying the molecular weight of the flexible propylene oxide diamine while keeping the molecular weight of the rigid diamine constant. At small values of ΔT_g, a single T_g is observed for the mixed epoxy formulations, with no detectable broadening of the transition. At intermediate ΔT_g values, the cured formulation exhibits nanoscale structure and two overlapping T_g's, from both a DGEBA/rigid diamine rich phase and a DGEBA/flexible diamine rich phase, where the T_g values in rigid and flexible phase are shifted from the respective homogeneous single diamine T_g due to segmental-level interactions between the two diamines. At the largest ΔT_g values, two distinct T_g's are observed, along with macroscale phase separation. The T_g's of the rigid and flexible phase are only slightly shifted from the respective neat components for this largest ΔT_g system. The effect of dynamic heterogeneity on the ballistic performance is also compared to a model structural epoxy to highlight the utility of dynamic and structural heterogeneity.

EXPERIMENTAL

The chemical structures of the materials used in this study are shown in Figure 1. Diglycidyl ether of bisphenol-A (DGEBA, or EPON825) was purchased from Miller-Stephenson. The rigid diamine 4,4′-methylenebis(cyclohexylamine) (PACM) was provided by Air Products. The flexible propylene oxide-based Jeffamine diamines: D230, D400, D2000, and D4000 were purchased from Huntsman. All materials were used as received without further purification.

Stoichiometric mixtures of DGEBA with the diamines were prepared and the fraction of amine hydrogens from PACM was varied from 0 (DGEBA cured with only Jeffamine) to 1 (DGEBA cured with only PACM) for each Jeffamine series. Samples were prepared by preheating monomers to 60 °C in appropriate amounts for a given composition in a nitrogen-purged oven. Mixing was performed over the course of approximately 3 minutes with a high speed blade mixer. After mixing, the systems were degassed under vacuum, then transferred to preheated stainless steel molds which had been coated with a mold-release agent. Curing was carried out within a nitrogen-purged oven for 2 h at 80 °C, 8 h at 150 °C, followed by a post-cure at 200 °C for 2 h.

The morphology of select compositions was imaged using a laser scanning microscope, which was performed on a Keyence VK-X200 with a 100× objective. Fracture surfaces from ballistic impact specimens were imaged.

Dynamic mechanical analysis (DMA) was performed on a Q800 DMA from TA Instruments. Single cantilever mode was used. Samples were measured with a constant displacement of 7.5 to 10 microns at a frequency of 1 Hz on heating from −130 °C to 200 °C. The sample thickness was adjusted such that the resulting normal force for a given displacement was approximately the middle of the DMA manufacturer's prescribed range. This was typically done by preparing a ∼1 mm thick sample for sub-T_g measurements and a 3-6 mm thick sample for measurements at temperatures greater than T_g. Prior to the start of the DMA measurements, calibrations were performed to account for the machine compliance.

For select compositions, dielectric relaxation spectroscopy (DRS) was performed on a Novocontrol Concept 40 impedance analyzer system. Parallel-plate capacitor samples were prepared by sputter-coating 30 mm diameter gold-palladium electrodes onto thin films with a Denton Vacuum Desk V sputter unit. Samples were measured from −150 °C to well above the T_g of the material isothermally in 5 degree increments. Equilibration times of 15 minutes prior to the start of each frequency sweep were used to ensure thermal stability. Temperature was controlled by heating evaporated liquid nitrogen and passing it over the sample in a vacuum-insulated chamber. At each temperature, 64 frequencies were measured, evenly spaced on a logarithmic scale within the range of 10 MHz to 10 mHz. At each frequency point, a reference measurement was performed to improve accuracy. After the initial measurement, samples were re-measured at select temperatures to ensure no changes in the dynamics had occurred. The in-phase (ε') and out-of-phase (ε'') components of the complex dielectric constant ($\varepsilon^\star = \varepsilon' - i\varepsilon''$) were calculated at each frequency point from the measured impedance and the sample geometry.

The room-temperature (22 °C) ballistic performance of these materials was evaluated on a gas gun firing a spherical 5.56 mm diameter, 0.69 gram, 302 stainless steel projectile. The projectile velocity was tracked with a Doppler radar system. Samples, 60 mm × 60 mm × 6.4 mm, were clamped in an aluminum frame with a ∼51 mm diameter aperture. A sheet of 0.05 mm thick, type 2024-T3 aluminum foil was placed 50 mm behind the impacting surface of the sample. During testing, any penetration of the aluminum foil, either by the projectile, or by a fragment of the epoxy sample was considered a penetration event. The KE50 is calculated by averaging the three highest kinetic energy non-penetrating shots and the three lowest kinetic energy penetrating shots. For clarity, the KE50 values
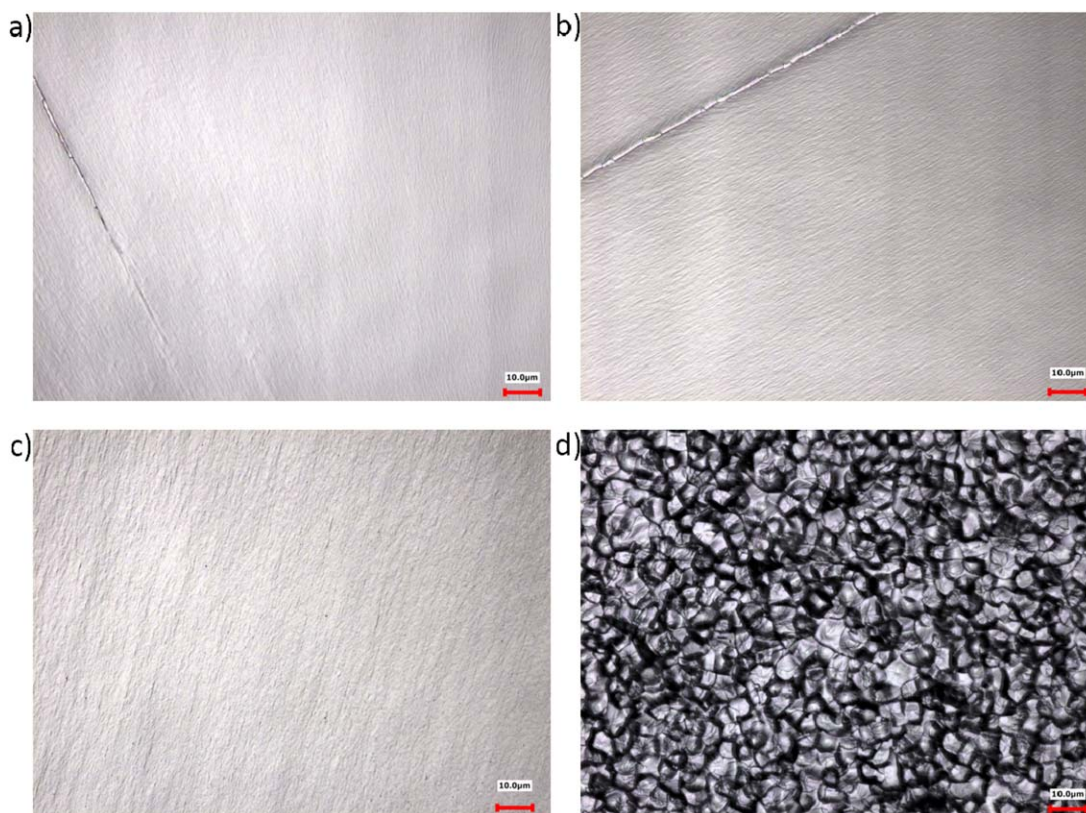
Figure 2. Laser scanning microscope images of ballistic fracture surfaces of (a) DGEBA/PACM/D230 at $X = 0.5$, (b) DGEBA/PACM/D400 at $X = 0.5$, (c) DGEBA/PACM/D2000 at $X \sim 0.8$, and (d) DGEBA/PACM/D4000 at $X = 0.8$. Scale bars are 10 microns. [Color figure can be viewed in the online issue, which is available at wileyonlinelibrary.com.]

presented here are normalized by the KE50 of DGEBA cured with Jeffamine D4000.

RESULTS AND DISCUSSION

Shown in Figure 3 are the DMA results for each of the blend systems investigated. For DGEBA crosslinked with either the PACM/D230 or the PACM/D400 series of mixtures, the transition between the glassy and rubbery state in the E' data occurs over a narrow temperature range and gradually increases to high temperatures with increasing PACM content. Tan δ for both the DGEBA/PACM/D230 and DGEBA/PACM/D400 systems shows a single peak indicative of a homogeneous network with a single glass transition temperature. These materials are optically transparent, as shown in Figure 2. The DGEBA/PACM/D2000 blends, also shown in Figure 2, are optically transparent and exhibit a broad transition region between the glassy and rubber state in E'. However, tan δ shows multiple overlapping peaks indicative of a heterogeneous network with multiple transitions. Indeed, previous results showed that these DGEBA/PACM/D2000 formulations exhibit dual transitions corresponding to a unique T_g from each component including a DGEBA/D2000 rich phase and DGEBA/PACM rich phase.[26] Large shifts in the pure component T_g's (for example stoichiometric DGEBA/PACM or stoichiometric DGEBA/D2000) due to fine mixing of the diamines was observed, along with the development of nanoscale structure which was found to be beneficial to the ballistic performance. Previous research has shown that

DGEBA/PACM/D4000 blends at high PACM content ($X > 0.9$) are opaque.[26] The DGEBA/PACM/D4000 compositions investigated here exhibit strong phase separation at $X > 0.5$, evident in both the DMA scans [Figure 3(d,h)], and in the opacity of most blend compositions, as shown in Figure 2(d), exhibiting phase separation on the order of 5 microns to 10 microns. The DMA results suggest the PACM-rich phase and the D4000-rich phase are only slightly perturbed relative to the neat homogeneous resins. This suggests that while some segmental-level mixing does occur, these mixed DGEBA/PACM/D4000 formulations are largely heterogeneous.

The ΔT_g, differences in pure component T_g's (for example stoichiometric formulations of DGEBA/PACM, DGEBA/D230, DGEBA/D400, DGEBA/D2000, or DGEBA/D4000), taken as the peak in tan δ from the DMA scans, are shown in Figure 4. The increase in ΔT_g with increasing Jeffamine molecular weight follows the expected trend of a decreasing T_g of the DGEBA/Jeffamine with the increasing Jeffamine molecular weight. This trend also agrees with the observation that T_g increases with increasing crosslink density, which in the series of Jeffamines examined here, occurs due to the differences in molecular weight.

In order to verify that only a single T_g is present in the DGEBA/PACM/D230 and DGEBA/PACM/D400 mixtures, a single composition from each blend series was selected for dielectric spectroscopy measurements. The conductivity-free dielectric loss (ε_D'') at 1 Hz is shown in Figure 5 for the blends of DGEBA/PACM/D400

Figure 3. Storage modulus (a–d) and Tan δ (e–h) versus temperature for (a,e) D230 blends, (b,f) D400 blends (c,g) D2000 blends, and (d,h) D4000 blends. Data in (g) are reproduced from Ref. 26. [Color figure can be viewed in the online issue, which is available at wileyonlinelibrary.com.]
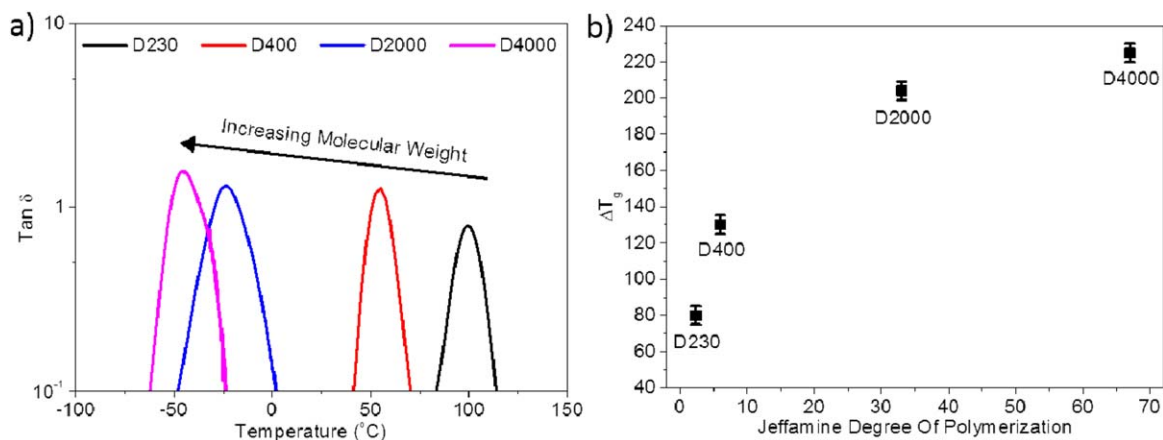
Figure 4. (a) Tan δ as a function of temperature for DGEBA cured with stoichiometric amounts of either D230, D400, D2000, or D4000, and (b) the difference in T_g between pure DGEBA/PACM and pure DGEBA/Jeffamine as a function of the Jeffamine molecular 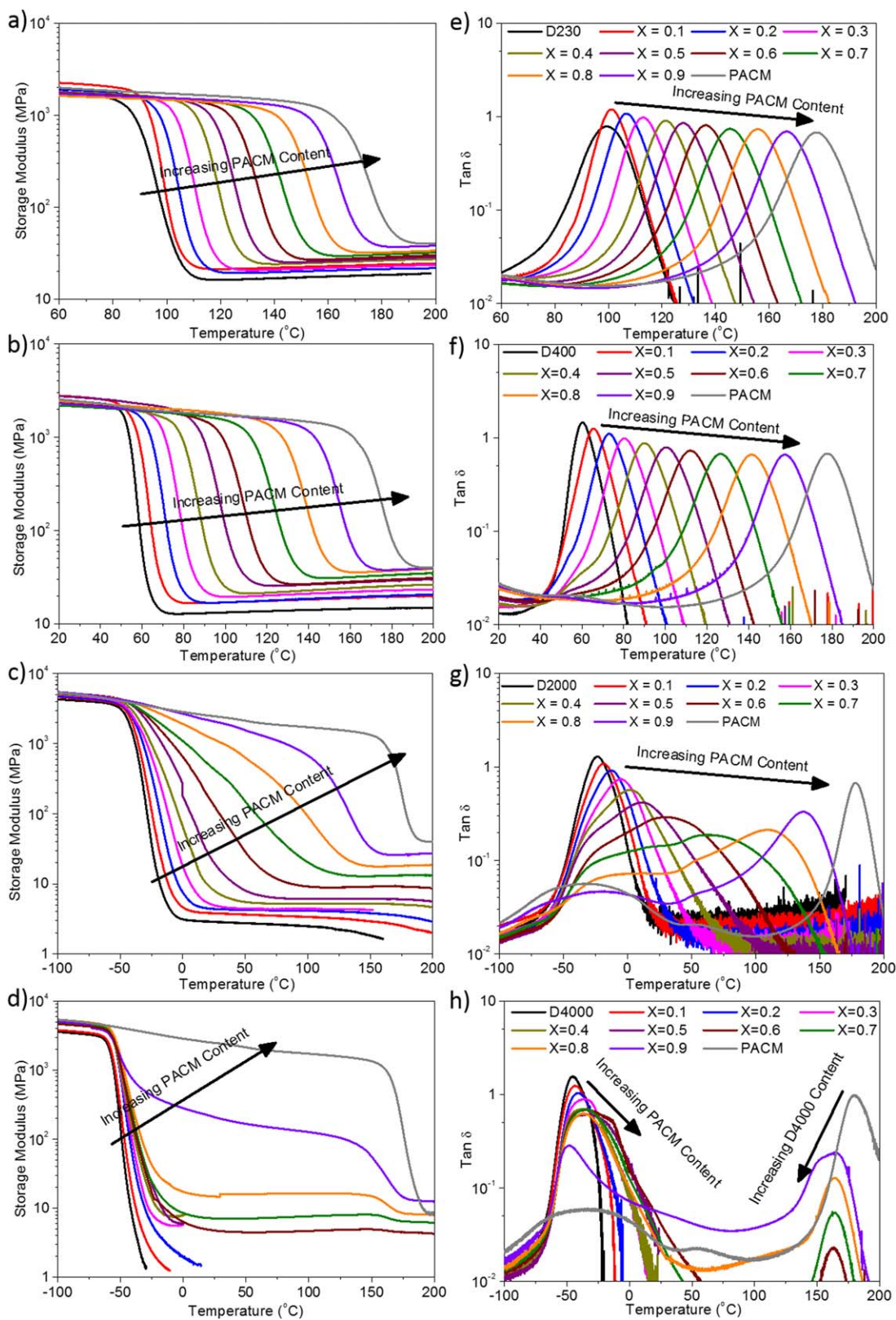weight. The T_g is taken as the peak in Tan δ from DMA scans. [Color figure can be viewed in the online issue, which is available at wileyonlinelibrary.com.]

($X = 0.67$) and DGEBA/PACM/D230 ($X = 0.52$), as well as neat DGEBA/PACM, neat DGEBA/D400, and neat DGEBA/D230. The "X" values for the mixed diamine systems were chosen so that the volume fraction of the PACM and Jeffamine were equivalent in the formulation. The conductivity-free dielectric loss has been shown to be particularly well-suited to the separation of multiple overlapping relaxations[27–29] often missed by techniques such as DMA and DSC. The details of the analysis are provided in the literature.[30] For the DGEBA/PACM/D400 and DGEBA/PACM/D230 mixtures, a single clear peak is observed due to the T_g of the these epoxy formulations. At higher temperatures, a characteristic upturn due to charge accumulation at the blocking electrodes is observed. This upturn has been removed from the neat DGEBA/D400, DGEBA/D230, and DGEBA/PACM samples for clarity. The peak for the DGEBA/PACM/D400 and DGEBA/PACM/D230 diamine mixture lies approximately midway between the neat components, which is expected since the volume fraction of each

diamine is the same. In agreement with the scaled DMA results shown below, the breadth of the DGEBA/PACM/D400 and DGEBA/PACM/D230 relaxation peaks is approximately the same as the neat components.

To better examine the effects of blending on the breadth of the glass transition, the tan δ curves for each system were normalized by the approximate peak in tan δ. These curves are shown in Figure 6. For both the DGEBA/PACM/D230 and the DGEBA/PACM/D400 mixtures, little or no broadening of the glass transition is observed, as shown in Figure 6(a,b) respectively. For the DGEBA/PACM/D2000 systems,[26] a T_g is observed for the PACM rich phase, and a second T_g is observed for the D2000 rich phase, as shown in Figure 6(c). Although difficult to quantify, the peaks corresponding to the PACM and the D2000 rich T_g's do appear to be broadened as well as overlapped significantly for most blend compositions. For the DGEBA/PACM/D4000 systems, the dynamic heterogeneity is greatest, and both the PACM rich T_g and the D4000 rich T_g are well-separated in the mixtures. Shown in Figure 6(d) is the normalized tan δ peak for the D4000 rich phase of the DGEBA/PACM/D4000 formulation. Of interest is the broadening observed for each of the PACM/D4000 compositions, suggesting that while most of these systems undergo macroscale phase separation, some amount of segmental-level mixing occurs. The normalized tan δ peak of the PACM rich phase for the DGEBA/PACM/D4000 systems is shown in Figure 6(e). Due to phase angle limitations of the DMA used, the PACM T_g could not be measured at $X = 0.5$ and below. With the exception of the $X = 0.9$ composition, the PACM tan δ peak does not appear to be broadened in these mixtures.

The Fox-Flory equation can be used to describe the compositional dependence of intimately mixed systems which exhibit a single T_g following a simple rule of mixtures. In eq. (1), w_1 and w_2 are the weight fractions of components 1 and 2, respectively.

$$\frac{1}{T_g} = \frac{w_1}{T_{g1}} + \frac{w_2}{T_{g2}} \qquad (1)$$

The Gordon-Taylor equation[31] is one of several slightly more complicated models which is used to describe the compositional dependence of T_g when a simple rule of mixtures (Fox-Flory) is
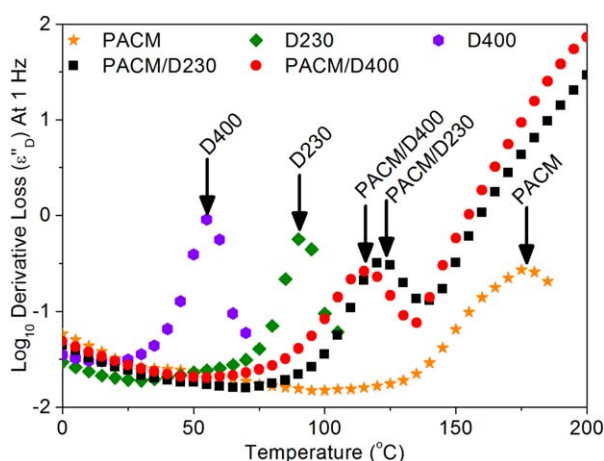
Figure 5. Derivative dielectric loss (ε_D'') versus temperature at 1 Hz for PACM (orange stars), D230 (green diamonds), D400 (purple hexagons), PACM/D230 ($X = 0.52$, black squares), and PACM/D400 ($X = 0.67$, red circles). The approximate peak locations are indicated for each sample by black arrows. [Color figure can be viewed in the online issue, which is available at wileyonlinelibrary.com.]
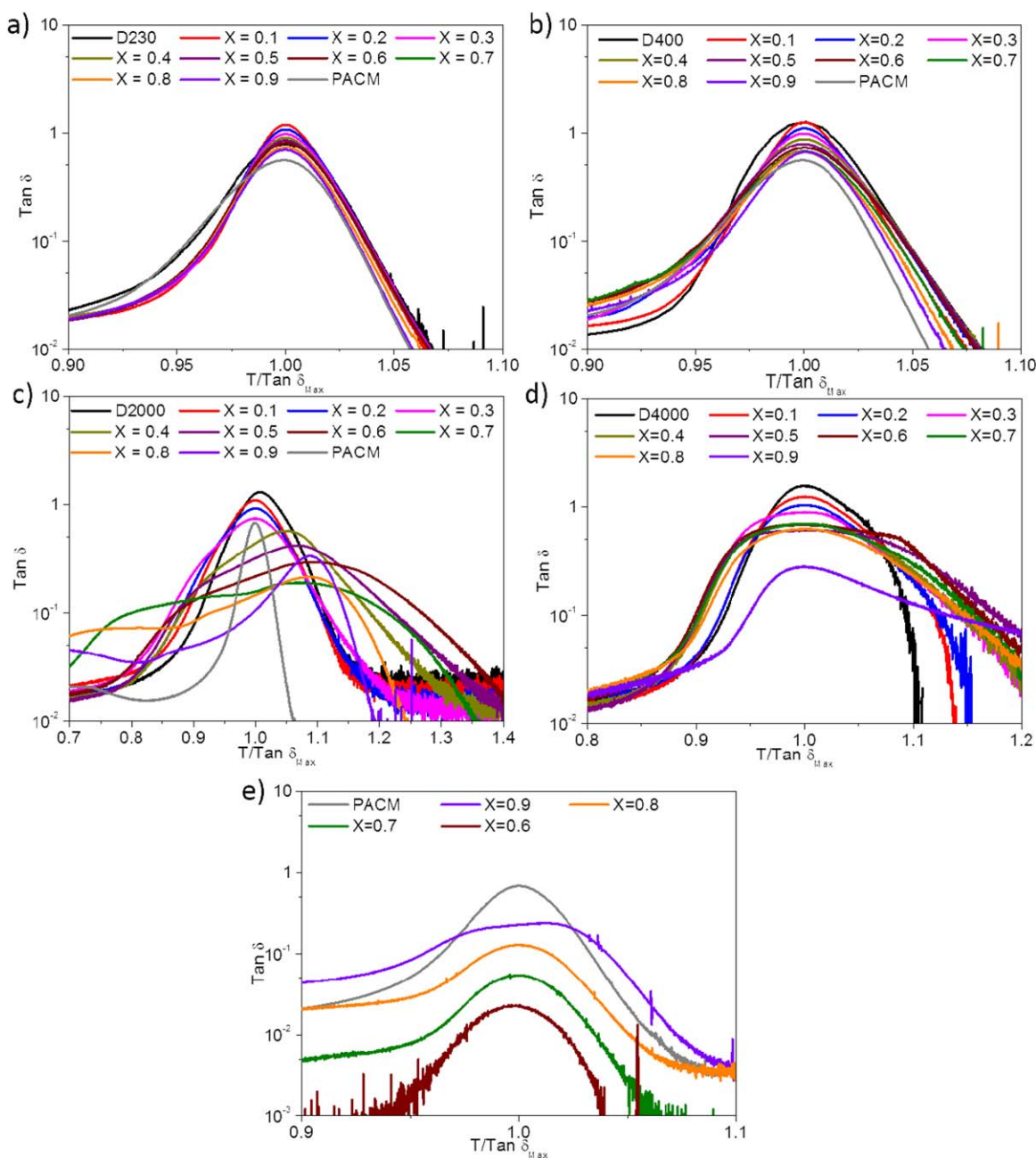
Figure 6. DMA data normalized by the peak temperature of the Tan δ plot or the average peak temperature for (a) D230, (b) D400, (c) D2000, (d) the D4000 peak of the D4000 blends and (e) the PACM peak of the D4000 blends. Data in (c) are reproduced from Ref. 26. [Color figure can be viewed in the online issue, which is available at wileyonlinelibrary.com.]

insufficient. In eq. (2), k is an adjustable parameter, while w_1 and w_2 are the same as in eq. (1).

$$T_g = \frac{w_1 T_{g1} + k * w_2 T_{g2}}{w_1 + k * w_2} \qquad (2)$$

Shown in Figure 7 is the compositional dependence of T_g (or T_g's) for each blend system investigated. The red and blue lines in Figure 7 represent the prediction of the Fox-Flory equation, along with fits of the Gordon-Taylor equation, respectively. Considering only the intimately mixed DGEBA/PACM/D230 and DGEBA/PACM/D400 systems exhibiting a single T_g (single tan δ peak and single dielectric loss peak), the Fox-Flory equa-

tion predicts the compositional dependence of T_g reasonably well, but not perfectly. However, the Gordon-Taylor fits are excellent, with k values of 1.698 for the DGEBA/PACM/D230 blends and 1.359 for the DGEBA/PACM/D400 blends. Since w_1 and w_2 are the weight fraction of a stoichiometric DGEBA/ PACM and DGEBA/Jeffamine component in the formulation, respectively, this suggests that these D230 and D400 blends with PACM are well mixed.

In contrast, both the DGEBA/PACM/D2000 and the DGEBA/ PACM/D4000 systems exhibit stronger dynamic heterogeneity. Both a PACM-rich T_g and a D2000 (or D4000)-rich T_g are
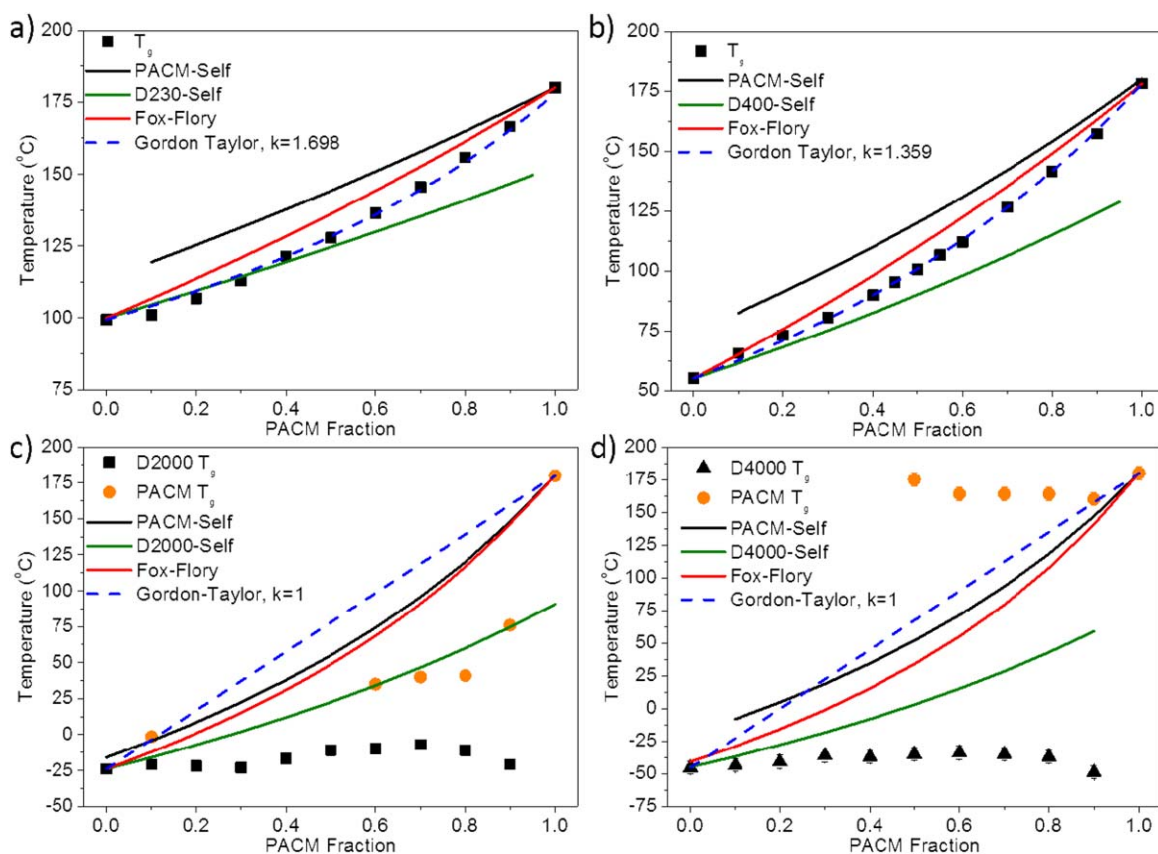
Figure 7. Compositional dependence of T_g for the (a) D230, (b) D400, (c) D2000, and (d) D4000 systems. PACM self-concentration (black line), Jeffamine self-concentration (green lines), Fox-Flory (red solid line), and Gordon-Taylor (blue dashed line) predictions are also shown. Values of the Gordon-Taylor k-parameter are listed in the legends. [Color figure can be viewed in the online issue, which is available at wileyonlinelibrary.com.]

observed in each blend composition. In particular, the D4000 blends exhibit strong phase separation, phase separating into opaque samples for most compositions. The DMA data in Figure 2 shows that both the PACM rich and D2000 rich phase in the DGEBA/PACM/D2000 mixed formulations exhibit sizable shifts in T_g when compared to the stoichiometric DGEBA/PACM and DGEBA/D2000 homogeneous resins, respectively, suggesting more intimate mixing of the diamines within the formulation. The DGEBA/PACM/D2000 mixtures are classically miscible in the sense of maintaining optical transparency across the compositional range. The presence of dual T_gs is typically an indicator of immiscibility, but this is not always the case.[20] Both the Fox-Flory prediction and the Gordon-Taylor fit with $k = 1$ fail to describe the compositional dependence of the PACM rich phase T_g and the D2000 rich phase T_g.

The DGEBA/PACM/D4000 mixtures exhibit only small changes in the T_g of each phase with composition, being even more strongly phase separated than the D2000 blends, owing to their greater degree of polymerization and the associated entropic penalty to mixing as the network molecular weight increases. In these blends, both the Fox-Flory and the Gordon-Taylor equations fail to capture the compositional dependence of T_g. The PACM T_g does decrease slightly with the addition of D4000, particularly for the $X = 0.9$ composition, which suggests

some amount of mixing, and is reflected in the DMA results shown in Figure 3(e). The changes in the PACM T_g are at most 20 °C, and again reflect the gross phase separation visually observed for these samples. It is not clear if it is appropriate to model the DGEBA/PACM/D2000 and DGEBA/PACM/D4000 mixtures with the Fox-Flory, Gordon-Taylor, or any other model of the compositional dependence of T_g. In particular, the DGEBA/PACM/D4000 blends are classically phase separated by nearly every measure of miscibility, so it is unsurprising such models fail to capture subtle changes in the T_g of each phase.

Also included in each of the plots in Figure 7 are predictions of the effective T_g of the PACM component (black lines) and the Jeffamine component (green lines) using the Lodge-McLeish model.[25] The Lodge-McLeish model, and similar work by Painter and Coleman[32–35] examines the effects of concentration fluctuations or local dynamic heterogeneity which are a result of chain connectivity. The model uses a modified Fox-Flory equation, with ϕ being the volume fraction of component A or B:

$$\frac{1}{T_g(\phi)} = \frac{\phi_{effective}}{T_{g,A}} + \frac{1-\phi_{effective}}{T_{g,B}} \qquad (3)$$

The effective T_g for a given component is then calculated assuming an effective volume fraction, modified from the global volume fraction due to chain connectivity effects.
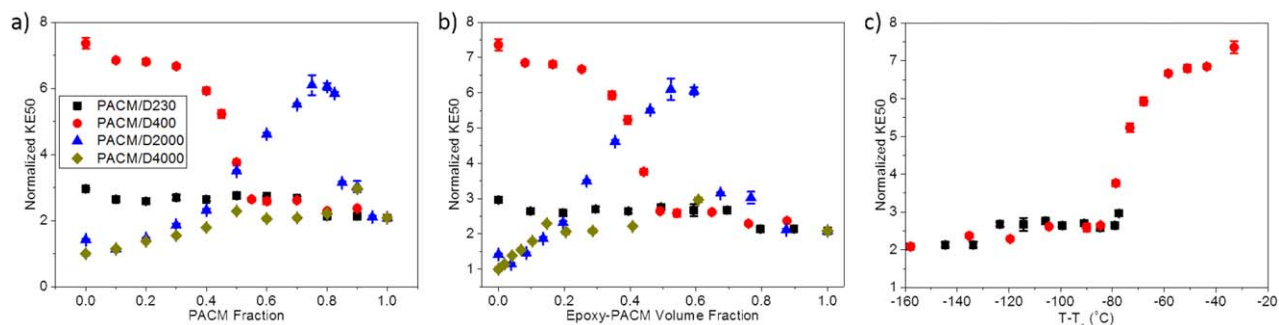
Figure 8. Room-temperature normalized KE50 values for each of the blend systems. DGEBA/PACM/D230 (squares), DGEBA/PACM/D400 (circles), DGEBA/PACM/D2000 (triangles), DGEBA/PACM/D4000 (diamonds) as a function of (a) PACM fraction, (b) Epoxy-PACM volume fraction, and (c) T-T_g. DGEBA/PACM/D2000 data in (a) and (b) are reproduced from reference 26. [Color figure can be viewed in the online issue, which is available at wileyonlinelibrary.com.]

$$\phi_{effective} = \phi_{self} + \left(1 - \phi_{self}\right)\phi \qquad (4)$$

In their initial paper, Lodge and McLeish assume a hypothetical miscible mixture of a rigid and a flexible component with T_g's of 200 °C and 100 °C, respectively. To this hypothetical blend, they assigned a self-concentration value of 0.2 and 0.3 for the rigid and flexible components, respectively, based on results for real systems. This hypothetical system, while likely assuming a mixture of two high molecular weight thermoplastics, is similar to the blends investigated here, in particular the DGEBA/PACM/D230 systems: a mixture of rigid PACM and flexible Jeffamines. In particular, this hypothetical system closely matches the DGEBA/PACM/D230 mixtures, where the neat components: DGEBA/D230 and DGEBA/PACM exhibit T_g's of 100 °C and 180 °C, respectively. The model does not explicitly account for the effects of specific interactions such as hydrogen bonds, which are present in these systems. Hydrogen bonding should, however, only occur in the Jeffamine phase between hydroxyl groups formed during curing and the Jeffamine ether oxygens.

Applying a self-concentration value of 0.2 to PACM and 0.3 for each of the Jeffamines, the black and green curves of each plot in Figure 7 are returned. For the D230 system, the predicted effective T_g of the D230 component from the Lodge-McLeish model appears to describe the compositional dependence of the mixture T_g at low D230 contents. This is not the case for the D400 blends with PACM. The D2000 blends are an interesting system, since the materials exhibit very fine phase separation, on the order of a few nanometers, and exhibit dual T_g's. The DGEBA/PACM/D2000 series may be a useful system to evaluate the applicability of self-concentration models such as the Lodge-McLeish and the TFT, since the spatial heterogeneity in these mixtures is known, and approaches the monomer size. The Lodge-McLeish model does appear to describe the T_g of the PACM phase for the $X = 0.1$ blend quite. The agreement of the D2000 self-concentration curve with the PACM T_g is interesting, but is likely a simple coincidence. This blend was previously found to exhibit nanometer-scale phase separation, with a length scale near 2–5 nanometers, or approximately one radius of gyration for the D2000 molecule. This, along with the small invariant value (see Ref. 26), suggests D2000 very finely dispersed within the PACM matrix, and may be appropriately

described by this model. In the D4000 mixtures, the ϕ values chosen for the Lodge-McLeish model may not be strictly appropriate, due to the macroscale phase separation, which should yield a ϕ_{self} value near unity for both components.

For a more accurate prediction of the component T_g's, an additional correction would need to be introduced to account for the different Jeffamine chain lengths. In these systems, we hypothesize self-concentration of the Jeffamines occurs due to two processes: phase separation as the network molecular weight develops, and the molecular weight of the Jeffamine creating a larger volume of that chemical species before another PACM monomer is encountered. Even if phase separation were favorable in the D230 and D400 blends with PACM, phase separation cannot occur with the development of molecular weight due to the kinetic trapping and the reduced entropic penalty of mixing relative to the D2000 and D4000 components. In the D2000 system, the entropic penalty occurs at an earlier stage of cure, but phase separation on the order of less than 10 nanometers occurs prior to kinetic trapping. If the cure temperature of the DGEBA/PACM/D2000 systems is modified to gel at lower temperatures, the mixtures have been observed to macrophase separate. In the D4000 case, the larger degree of polymerization causes the materials to phase separate at early stages of cure, forming large domains. A more thorough analysis of the effects of self-concentration in these systems would require determining the molecular persistence length, but the values used by Lodge and McLeish do appear to provide some insight.

The ballistic performance of the various mixtures is shown in Figure 8. The KE50 values were normalized to that of neat DGEBA/D4000 for clarity. The ballistic performance of the DGEBA/PACM/D230 blends increases slightly with increasing D230 content. The ballistic performance of the DGEBA/PACM/D400 blends does not obey a simple rule of mixtures, but rather passes through a sharp reduction in performance between a PACM fraction of 0.4 to 0.55. This transition does not mimic the compositional dependence of T_g as shown in Figure 7(b), nor do the DMA results shed any insight into why these mixtures behave in this manner. One hypothesis is that the mixtures transition from a continuous D400 matrix to a PACM matrix, resulting in a loss of ductility and a reduction in fracture toughness which are known to govern critical crack
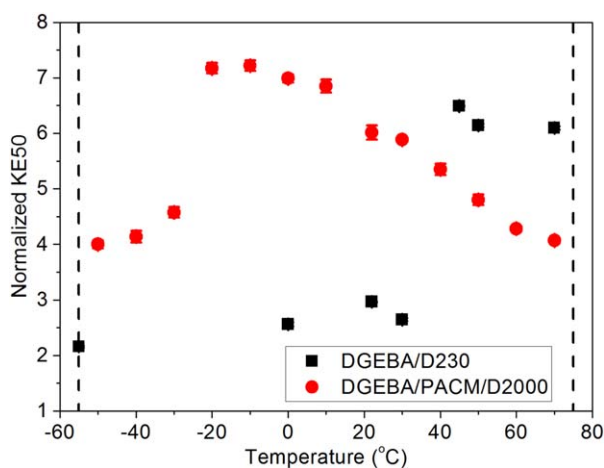
Figure 9. Normalized KE50 versus temperature for DGEBA/D230 and DGEBA/PACM/D2000 with $X \sim 0.8$. Dashed lines indicate the relevant Army temperature range. [Color figure can be viewed in the online issue, which is available at wileyonlinelibrary.com.]

formation.[3] At a PACM fraction of 0.55 and below, the volume fraction of D400 is greater than the volume fraction of PACM. This is shown more clearly in Figure 8(b), where the normalized ballistic performance is plotted versus the volume fraction of DGEBA with PACM. Below 50 volume % DGEBA with PACM, a sharp increase in ballistic performance occurs. This transition suggests that a critical factor for improving the ballistic performance of epoxy networks is the presence of a continuous ductile phase. The single T_g observed in the DGEBA/PACM/D400 system suggests that heterogeneity in this system is on the order of the monomer length scale and does not give rise to structural heterogeneity.

Another possibility is the temperature dependence of the ballistic performance relative to T_g. Shown in Figure 8(c) is the DGEBA/PACM/D400 and DGEBA/PACM/D230 ballistic data normalized by T-T_g, where T_g is taken as the maximum in tan δ from the DMA data. Both blend systems match the general temperature dependence previously observed for a broad range of epoxy networks.[36]

This transition from PACM rich to Jeffamine rich occurs below a PACM fraction of 0.5 for the DGEBA/PACM/D230 mixtures, but pure DGEBA/PACM and pure DGEBA/D230 both exhibit similar high glass transition temperatures and similar low KE50 values, so no transition in impact performance was observed in the DGEBA/PACM/D230 mixtures and they nominally follow a rule of mixtures. The ballistic performance of the DGEBA/PACM/D2000 blends has been previously investigated,[26] and has been found to depend on the nanoscale structure which develops during the curing process. However, the DGEBA/PACM/D2000 blends provide additional support for the hypothesis that a continuous ductile phase can be beneficial for high rate impact resistance, as Figure 8(b) shows that the maximum in KE50 occurs when the volume fraction of ductile D2000 is between 0.4 and 0.6, where continuity of the D2000 phase would be expected. Additional support for this hypothesis is from preliminary temperature dependent ballistic data on the

DGEBA/PACM/D2000 system shown in Figure 9. With a PACM content of $X = 0.8$ (epoxy-PACM volume fraction of 0.6) the KE50 of DGEBA/PACM/D2000 falls dramatically when the formulation is cooled below the glass transition temperature of the ductile D2000 rich phase, further reinforcing that not only is an interconnected structure key, but ductility in one of the phases is also important. As with the DGEBA/PACM/D230 blends, the ballistic performance of the DGEBA/PACM/D4000 blends approximately follows a rule of mixtures, with the exception of the $X = 0.5$ through $X = 0.9$ blends. A possible explanation for the observed increase in KE50 for these mixtures is the subtle depression of the PACM component T_g, which is likely due to some segmental-level mixing between the PACM and D4000 monomers at the early stages of cure. The $X = 0.9$ mixture is near 50 volume-% total amines (PACM + D4000), which may improve the ballistic performance due to a possible phase inversion morphology. The improved ballistic performance of this blend may also be due to the shifts in the PACM and the D4000 T_g's observed in the DMA results [Figures 3(d,h) and Figure 6(d,e)]. A clear high-temperature tail is observed on the D4000 peak, along with what appears to be a double peak for the PACM peak. This also suggests some segmental-level mixing does occur at this composition, although it is not clear why this would not occur at each DGEBA/PACM/D4000 composition. The DGEBA/PACM/D4000 data is interesting because despite going through a possible phase inversion as the fraction of rigid PACM decreases, the ballistic impact resistance does not improve substantially. Due the large scale of the DGEBA/PACM/D4000 phase separated morphology, this illustrates that a small scale morphology rather than macroscale is better for high rate impact resistance.

Many military applications require an operational temperature range of approximately −55 °C to 75 °C. The ballistic performance of DGEBA/D230 and DGEBA/PACM/D2000 ($X \sim 0.8$) are shown in Figure 9. Again, these values are normalized to pure DGEBA/D4000 for clarity. DGEBA/D230 is a structural epoxy, with a T_g (100 °C) well above the military operational range. It is used here as a comparison, since its ballistic response is typical of high T_g, structural epoxies. Below approximately 40 °C, however, the ballistic performance of this material is relatively poor, exhibiting brittle failure with extensive radial and cone cracking, as well as the ejection of fragments at the impact site. The DGEBA/PACM/D2000 blend exhibits a ballistic performance of at least 4x that of DGEBA/D4000 over the entire temperature window. While the ballistic performance suffers at elevated temperatures, the dynamically heterogeneous system performs 2–3.5 times better than the structural epoxy from 30 °C to −60 °C. This suggests that some degree of dynamic heterogeneity may result in dramatic improvements in ballistic performance through the use of a ductile component. The magnitude of this improvement highlights the utility of combined structural and dynamic heterogeneity for ballistic applications.

The improved ballistic performance of mixed hard and soft amines does, however, come at the expense of a greater temperature dependence of stiffness than a structural epoxy, as shown in Figure 10. The structural epoxy DGEBA/D230 exhibits a reduction in storage modulus from approximately 2.9 GPa to
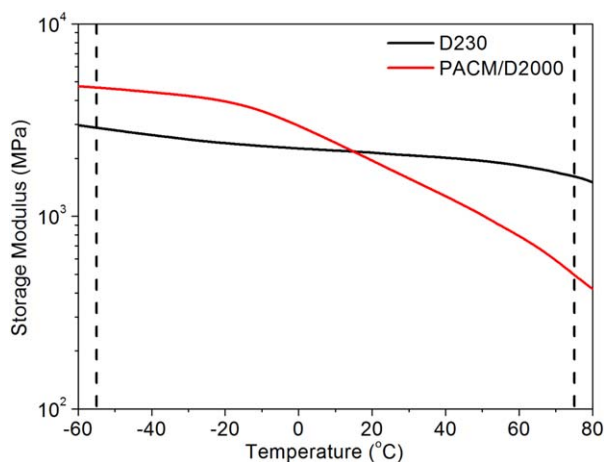
Figure 10. DMA storage modulus for DGEBA/D230 and DGEBA/PACM/D2000 with 50 volume % amines. Dashed lines indicate the relevant Army temperature range. [Color figure can be viewed in the online issue, which is available at wileyonlinelibrary.com.]

1.6 GPa, a drop of 45%. The DGEBA/PACM/D2000 sample exhibits a drop in storage modulus from 4.6 GPa to 0.5 GPa, or a drop of 90%. From 0 °C to 40 °C, however, the change in modulus is somewhat less. This trade-off of improved ballistic performance for a reduction in structural performance must be considered when designing an application. If, however, the structural requirements for the specific protection applications modest, a significant improvement in ballistic performance can be realized through the use of dynamically heterogeneous systems. Recently investigated thermosetting resins have been shown to exhibit both excellent ballistic performance and structural performance over the entire military temperature range.[37] These ring-opening metathesis polymerized resins, while potentially useful, still require investigations of their physical/chemical aging and compatibility with commercial fibers to be utilized in fiber reinforced composite applications.

CONCLUSIONS

In our previous publication on DGEBA/PACM/D2000 blended epoxies,[26] we demonstrated that the room temperature ballistic impact resistance for the blended formulations was improved relative to the stoichiometric DGEBA/PACM or DGEBA/D2000 neat materials. Specifically, the DGEBA/PACM/D2000 blends were optically transparent yet, dynamically heterogeneous with two glass transitions including a rigid and flexible phase. In particular for these blends the impact performance was highest when the blend morphology was near a phase inversion point and exhibited a small characteristic length scale.

In this study, we expand on this previous research to systematically examine a detailed series of blended epoxy formulations composed of DGEBA that is crosslinked with a mixture of a rigid cycloaliphatic diamine (PACM) and a flexible polypropylene glycol based diamine (Jeffamine), where the Jeffamine molecular weight was varied from 230, 400, 2000, and 4000 g/ mole. We examined the influence of the flexible Jeffamine molecular weight and composition on the mechanical and thermal properties of the cured blends, as well as dynamic and

structural heterogeneity in these materials with a specific cure protocol. In particular we demonstrated the following key points:

- **The magnitude of the dynamic heterogeneity was controlled by controlling the molecular weight of the Jeffamine and therefore the effective ΔT_g for the blend system**, where ΔT_g is defined as the difference between the neat stoichiometric DGEBA/PACM T_g and DGEBA/Jeffamine T_g. A single T_g was observed for DGEBA/PACM/D230 and DGEBA/PACM/D400 mixtures having ΔT_g's of 80 °C and 130 °C, respectively. However, the DGEBA/PACM/D2000 blends ($\Delta T_g \sim 205$ °C) were dynamically heterogeneous, exhibiting two distinct T_g's, corresponding to a high T_g PACM rich phase and a low T_g D2000 rich phase. With the DGEBA/PACM/D2000 blends both the high T_g phase and low T_g phase exhibited a shift in T_g relative to the neat DGEBA/PACM and DGEBA/D2000, due to mixing between the rigid and soft phases. The DGEBA/PACM/D4000 mixtures exhibited the greatest dynamic heterogeneity ($\Delta T_g \sim 225$), and the PACM and D4000 components appear to be strongly phase separated, with only minimal changes in the component T_g's with composition, demonstrating minimal mixing between the two phases.
- **The ballistic impact resistance of the blended epoxies was strongly dependent on the extent of dynamic heterogeneity.** Specifically, for the non-heterogeneous single T_g DGEBA/ PACM/D230 and DGEBA/PACM/D400 blends, the temperature dependent ballistic penetration resistance simply correlated with the difference between the impact temperature and the resin T_g. These heterogeneous blends behaved similarly to non-blended epoxy resins[36] by exhibiting a sharp rise in penetration resistance when the measurement temperature is approximately 60 °C below the T_g. For the most dynamically heterogeneous DGEBA/PACM/D4000 blends, the ballistic performance was found to generally follow a rule of mixtures, and exhibited minimal improvements as a function of blend composition, likely due to the large length scale of the phase separation coupled with the poor intermixing between the high T_g and low T_g phase in these blends. In contrast, the dynamically heterogeneous DGEBA/PACM/D2000 blends, which were optically transparent, exhibited a strong deviation from rule of mixtures, with substantial improvements in the ballistic impact resistance relative to the neat components when the composition of the amine phase was approximately 50%.
- **Dynamically heterogeneous epoxy blends with a small scale structure offers the potential for new transparent resin formulations with impact resistance that can be improved over military operational temperature ranges.** The dynamically heterogeneous DGEBA/PACM/D2000 blends with an amine composition near 50% exhibited improved impact performance relative to model structural resins over military operational temperature ranges. The improved impact performance was accompanied by a stronger temperature dependent modulus. However, over most of the military temperature range the DGEBA/PACM/D2000 blends exhibited a similar modulus to the single T_g blends or a model structural

resin. Based on these results we conclude that homogeneous epoxy formulation composed of blended monomers offers minimal potential to exhibit improved impact performance and follow the same temperature dependent trends as single T_g non-blended formulations. However, dual glass transition blends, with a controlled ΔT_g between the individual components, offers the potential to improve impact resistance in extreme military temperature ranges as long as a ductile and rigid phase are both present at the impact temperature.

ACKNOWLEDGMENTS

REFERENCES

1. Sprenger, S. *J. Appl. Polym. Sci.* **2013**, *130*, 1421.

2. Ellis, B. Chemistry and Technology of Epoxy Resins, 1st ed.; Springer: Netherlands, **1993**.

3. Bain, E.; Knorr, D. Jr.; Richardson, A.; Masser, K.; Yu, J.; Lenhart, J. *J. Mater. Sci.* **2016**, *51*, 2347.

4. Dittanet, P.; Pearson, R. A. *Polymer* **2012**, *53*, 1890.

5. Kothmann, M. H.; Zeiler, R.; Rios de Anda, A.; Brückner, A.; Altstädt, V. *Polymer* **2015**, *60*, 157.

6. Sprenger, S. *Polymer* **2013**, *54*, 4790.

7. Choi, J.; Yee, A. F.; Laine, R. M. *Macromolecules* **2004**, *37*, 3267.

8. Ma, J.; Mo, M. S.; Du, X. S.; Dai, S. R.; Luck, I. *J. Appl. Polym. Sci.* **2008**, *110*, 304.

9. Miloskovska, E.; Hansen, M. R.; Friedrich, C.; Hristova-Bogaerds, D.; van Duin, M.; de With, G. *Macromolecules* **2014**, *47*, 5174.

10. Zhang, J.; Zhang, H.; Yan, D.; Zhou, H.; Yang, Y. *Sci. Chin. Ser. B: Chem.* **1997**, *40*, 15.

11. Jansen, B. J. P.; Rastogi, S.; Meijer, H. E. H.; Lemstra, P. J. *Macromolecules* **1999**, *32*, 6290.

12. Jajam, KC; Tippur, HV; Bird, SA; and Auad, ML. Dynamic Fracture and Impact Energy Absorption Characteristics of PMMA-PU Transparent Interpenetrating Polymer Networks (IPNs). In Dynamic Behavior of Materials, Volume 1; Song, B., Casem, D., and Kimberley, J., Eds. Springer International Publishing, **2014**; pp 277–284.

13. Blanco, M.; López, M.; De Arcaya, P. A.; Ramos, J. A.; Kortaberria, G.; Riccardi, C. C.; Mondragon, I. *J. Appl. Polym. Sci.* **2009**, *114*, 1753.

14. Chen, J. L.; Chang, F. C. *Macromolecules* **1999**, *32*, 5348.

15. Jayle, L.; Bucknall, C. B.; Partridge, I. K.; Hay, J. N.; Fernyhough, A.; Nozue, I. *Polymer* **1996**, *37*, 1897.

16. Oyanguren, P. A.; Frontini, P. M.; Williams, R. J. J.; Vigier, G.; Pascault, J. P. *Polymer* **1996**, *37*, 3087.

17. Wang, J.; Ye, L. *Compos. Part B-Eng.* **2015**, *69*, 389.

18. Zubeldia, A.; Larrañaga, M.; Remiro, P.; Mondragon, I. *J. Polym. Sci. Part B: Polym. Phys.* **2004**, *42*, 3920.

19. Hydro, R. M.; Pearson, R. A. *J. Polym. Sci. Part B: Polym. Phys.* **2007**, *45*, 1470.

20. Lodge, T. P.; Wood, E. R.; Haley, J. C. *J. Polym. Sci. Part B: Polym. Phys.* **2006**, *44*, 756.

21. Coleman, M. M.; Graf, J. F.; Painter, P. C. Specific Interactions and The Miscibility Of Polymer Blends; Taylor and Francis, **2003**.

22. Stanzione, J. F.; Strawhecker, K. E.; Wool, R. P. *J. Non-Crystalline Solids* **2011**, *357*, 311.

23. Wool, R. P. *J. Polym. Sci. Part B: Polym. Phys.* **2008**, *46*, 2765.

24. Wool, R. P.; Campanella, A. *J. Polym. Sci. Part B: Polym. Phys.* **2009**, *47*, 2578.

25. Lodge, T. P.; McLeish, T. C. B. *Macromolecules* **2000**, *33*, 5278.

26. Masser, K. A.; Knorr, D. B. Jr.; Hindenlang, M. D.; Yu, J. H.; Richardson, A. D.; Strawhecker, K. E.; Beyer, F. L.; Lenhart, J. L. *Polymer* **2015**, *58*, 96.

27. Masser, K. A.; Runt, J. *Macromolecules* **2010**, *43*, 6414.

28. Fragiadakis, D.; Pissis, P.; Bokobza, L. *Polymer* **2005**, *46*, 6001.

29. Fragiadakis, D.; Pissis, P. *J. Non-Cryst. Solid.* **2007**, *353*, 4344.

30. Wübbenhorst, M.; van Turnhout, J. *J. Non-Cryst. Solid.* **2002**, *305*, 40.

31. Gordon, M.; Taylor, J. S. *J. Appl. Chem.* **1952**, *2*, 493.

32. Coleman, M. M.; Pehlert, G. J.; Painter, P. C. *Macromolecules* **1996**, *29*, 6820.

33. Coleman, M. M.; Xu, Y.; Painter, P. C. *Macromolecules* **1994**, *27*, 127.

34. Painter, P.; Park, Y.; Coleman, M. *J. Appl. Polym. Sci.* **1998**, *70*, 1273.

35. Painter, P. C.; Coleman, M. M. *Macromolecules* **2009**, *42*, 820.

36. Knorr, D. B. Jr.; Yu, J. H.; Richardson, A. D.; Hindenlang, M. D.; McAninch, I. M.; La Scala, J. J.; Lenhart, J. L. *Polymer* **2012**, *53*, 5917.

37. Knorr, D. B. Jr.; Masser, K. A.; Elder, R. M.; Sirk, T. W.; Hindenlang, M. D.; Yu, J. H.; Richardson, A. D.; Boyd, S. E.; Spurgeon, W. A.; Lenhart, J. L. *Compos. Sci. Technol.* **2015**, *114*, 17.